Structures of a Periodically Excited Liquid Jet in a Non-dimensional Map

Frank Geschner, Humberto Chaves

Institute of Mechanics and Fluid Dynamics, Freiberg University of Mining and Technology,
Lampadiusstr. 4, 09596 Freiberg, Germany,
Frank.Geschner@imfd.tu-freiberg.de

ABSTRACT
The present study has been performed to obtain a better understanding of the atomization process. The strategy is first to minimize stochastic perturbations by generating a laminar jet and to reduce all other perturbations produced by the injection system to a minimum. In a second step well defined periodic velocity fluctuations are imposed on the jet by modulating the upstream pressure by a piezo-ceramic. The modulation produces a multitude of different, highly reproducible structures on the jet ranging from the prompt production of droplets at the nozzle exit through bell like shapes to finger like structures. This suggests that the coupling of internal flow to the spray formation near the nozzle is a deterministic process. A set of dimensionless parameters has been chosen by which a modulated jet can be characterized. The influence of these parameters on the shape of the structures has been determined. The result is a multi-dimensional map of defined regions in the dimensionless parameter space for the different structures observed.

INTRODUCTION

Atomization of liquid jets is of fundamental interest in many fields of industry and research. However, the atomization process is not well understood yet. It is well known that the atomization of a liquid, caused by exiting a nozzle, is influenced by the interaction with the surrounding air. This aerodynamic interaction has been studied extensively in the past both theoretically and experimentally. The theoretical method that has been applied is mainly linear stability theory. However, in reality finite perturbations generated already inside the nozzle initialize the atomization process. Therefore, a linear theory can only describe the effect of gas density. There are very few investigations of non-linear jet behaviour. For the case of an inviscid modulated jet Grabitz [1] obtained a solution of its kinematic behaviour that neglects the effects of surface tension and gas density. Nevertheless, this theory yields good agreement with many of the results obtained in the present paper. The main difficulty, both in experimental and theoretical work, is quantifying the frequency and the amplitude of disturbances introduced by the internal flow of the nozzle. In some technical applications injection is affected by modulation effects, e. g. due to pressure fluctuations. In most real situations, however, perturbations of the injection process are stochastic, e. g. due to turbulence. In the present investigation a different strategy is applied, i. e. defined finite perturbations are imposed on an otherwise undisturbed jet and the resulting jet morphology is studied.

PARAMETERS

The number of parameters needed to describe atomization can be reduced by dimensional analysis. The relevant physical parameters are the diameter of the nozzle exit D, the mean velocity of the jet $\bar{u}$, the density of the gas ϱ_{gas} wherein the jet is injected, the density of the test liquid ϱ_{liquid}, its surface tension σ, and its kinematic viscosity ν. The modulation parameters are the frequency f and the velocity fluctuation u'. Applying the Buckingham π-Theorem the following set of dimensionless parameters is suggested:

$$Sr = \frac{\pi D f}{\bar{u}}, \quad We_w = \frac{\varrho_{liquid}\bar{u}^3}{f\sigma}, \quad Re = \frac{D^2 f}{\nu}, \quad \varepsilon = \frac{u'}{\bar{u}}, \quad \varrho^* = \frac{\varrho_{gas}}{\varrho_{liquid}}. \tag{1a,b,c,d,e}$$

The special Weber-number We_w is obtained by dividing the ordinary Weber-number by the Strouhal-number The subscript w denotes the relation to the wavelength $\lambda = \bar{u}/f$ of the disturbance. This definition implies a much clearer map of the regions of appearance of the structures than the standard definition.

EXPERIMENTAL SET-UP

The experimental arrangement consists of three basic parts (Fig. 1): (i) a supply unit for the liquid (including a resonance chamber) with the possibility to vary the exit velocity of the jet, (ii) a convergent nozzle that minimizes the flow disturbances, and (iii) a recording unit consisting of an optical system, a CCD-camera and a PC with a frame-grabber-card for picture acquisition. The test liquid is excited by a piezo-ceramic oscillating in the ultrasonic range. The liquid is fed into the resonance space. Its upper wall is a movable piston which contains the piezo-crystal. Its adjustment makes it possible to achieve standing wave resonances. Thus the pressure fluctuations within the resonance space are intensified. To record the spatial and temporal development of the surface waves of the jet near the nozzle, the axis of the optics lies just below the nozzle exit. A high efficiency LED is used to illuminate the jet stroboscopically. The jet is imaged with a resolution of 315 pixel per millimetre. The dynamic behaviour of the set-up has been investigated both experimentally and theoretically. First the eigenmodes and the corresponding frequencies of the complete set-up were calculated numerically. These frequencies lie below the relevant modulation frequencies. However, there are two components of the set-up with resonances in the range of the modulation frequency: the convergent nozzle and the rod above the piezo-ceramic.

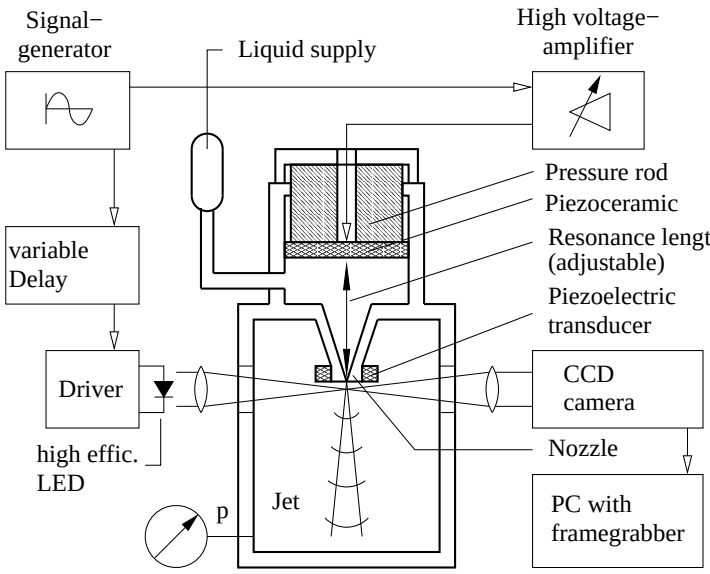

Figure 1: *Experimental set-up*

There is a strong vibrational coupling between the nozzle and the rod through the test fluid. The interaction between the two elements is complex as it depends on the supply pressure as well as on the frequency of modulation. However, the modulation amplitude of the jet is maximized at these discrete frequencies. Their measured values correspond to the resonance frequencies calculated. Since the structures observed are generated only at resonance, it is very difficult to quantify the modulation amplitude. A suitable method will be presented below. The chamber pressure as well as the supply pressure can be varied from atmospheric pressure up to $5\,MPa$. The frequency ranges from $20\,kHz$ to $120\,kHz$ in the present study. Since the large modulation amplitudes are only achieved at resonance the experiments are performed at five discrete frequencies. The dimensionless parameters were varied as follows: $0.74 < Sr < 17.42$, $5 < We_w < 28\,000$, $974 < Re < 4\,704$, $0.036 < \varepsilon < 0.8$ and $0.001\,2 < \varrho* < 0.012$.

INVESTIGATION OF THE MODULATION AMPLITUDE

With exception of $\bar{u}$ and u' all physical parameters can be measured directly. Prior to the experiments the properties of the test liquid were measured.

The mean velocity is obtained by measuring the difference between the supply and the chamber pressure. It is calibrated by the flow rate $\dot{V}(\Delta p, \zeta)$ measured at different supply pressures for atmospheric chamber conditions and used to calculate the unknown pressure loss factor ζ in a generalized Bernoulli equation

$$\dot{V}(\Delta p,\, \zeta) = A_{nozzle}\sqrt{\frac{2\Delta p}{\varrho\,[1+\zeta]}}. \tag{2}$$

For each flow rate the corresponding value for ζ can be determined. A linear function $\zeta(\Delta p)$ was sufficiently accurate to fit the measured data. This allows to calculate the mean velocity $\bar{u}$ on the basis of the measured pressure signals by dividing Eq. (2) by the nozzle area A_{nozzle}.

It is, however, much more difficult to determine the velocity fluctuation since the modulation frequency is in the ultrasonic range. The coupling factor between the driving voltage of the piezo-ceramic and the velocity fluctuation is strongly dependent on frequency and temperature and on the preloading of the piezo-ceramic.

A suitable theory has to be applied to obtain the correct coupling factor. Based on a theory by Grabitz [1] the development of the radius of the liquid jet along the jet co-ordinate can be described. For that purpose a one-dimensional inviscid unsteady flow is assumed and surface tension is neglected. In this case the conservation equations of momentum and mass simplify to

$$\frac{\partial u}{\partial t} + u\frac{\partial u}{\partial x} = 0, \tag{3}$$

$$\frac{\partial A}{\partial t} + u\frac{\partial A}{\partial x} + A\frac{\partial u}{\partial x} = 0. \tag{4}$$

with initial values at $x = 0$: $u = u_0(t)$, $A = A_{nozzle}$. u is the velocity in x-direction and A is the cross section of the jet. Lagrangian co-ordinates are introduced according to

$$\begin{aligned} t(\vartheta, \tau) &= \vartheta, \\ x(\vartheta, \tau) &= u_0(\tau)(\vartheta - \tau), \end{aligned} \tag{5}$$

leading to an exact solution of the initial value problem. Here τ is the time of exit of a fluid element from the nozzle and ϑ the time of observation. In the following dimensionless parameters are used where spatial co-ordinates are normalized by the radius of the nozzle r_0, velocities by the mean velocity at the nozzle exit $\bar{u}$ and times by $r_0/\bar{u}$. They are labeled by a tilde $\tilde{}$. When the output velocity at the nozzle exit is

$$\tilde{u}_0(\tau) = 1 + \varepsilon \sin(Sr\,\tilde{\tau}), \tag{6}$$

one obtains for the jet radius

$$\tilde{r}(\tilde{\vartheta}, \tilde{\tau}) = \sqrt{\frac{1 + \varepsilon \sin(Sr\,\tilde{\tau})}{\left|1 + \varepsilon \sin(Sr\,\tilde{\tau}) - \varepsilon\, Sr(\tilde{\vartheta} - \tilde{\tau}) \cos(Sr\,\tilde{\tau})\right|}}. \tag{7}$$

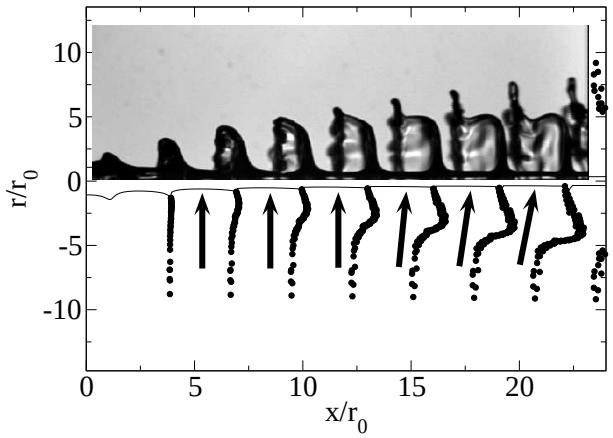

Figure 2: *Comparison between experimental data and calculated jet; $\bar{u} = 20.3\,m/s$, $\varepsilon = 0.2$, $f = 68\,kHz$*

Figure 2 shows a comparison of this theory with an experimental jet. Obviously the theory describes the jet profile very well near the minima of the jet radius. The influence of viscosity and surface tension is small at these positions. Therefore, these minima can be used to extract from the pictures the modulation amplitude and to calibrate the driving voltage by means of the theoretical model. The condition for extrema of Eq. (7) is

$$\begin{aligned} Sr\ [\varepsilon + \sin(Sr\,\tilde{\tau}_{min})] = \\ - \frac{\cos(Sr\,\tilde{\tau}_{min})\,[1 + \varepsilon\ \sin(Sr\,\tilde{\tau}_{min})]}{\tilde{\vartheta} - \tilde{\tau}_{min}}. \end{aligned} \tag{8}$$

This equation has to be solved for given $\tilde{\vartheta}$ and Sr. The resulting values for $\tilde{\tau}_{min}$ represent the exit time of fluid elements from the nozzle which are located at the minimum of the radius at the current time $\tilde{\vartheta}$. Physically meaningful values are $0 \le \tilde{\tau}_{min} < \tilde{\vartheta}$. Equation (7) can be rewritten in combination with Eq. (5) as

$$\frac{\tilde{r}(\tilde{\vartheta}, \tilde{\tau}_{min})_{min}^{-2} - 1}{\tilde{x}(\tilde{\vartheta}, \tilde{\tau}_{min})_{min}\, Sr} = \frac{\varepsilon\ \cos(Sr\,\tilde{\tau}_{min})}{\left[1 + \varepsilon\ \sin(Sr\,\tilde{\tau}_{min})\right]^2}. \tag{9}$$

The left hand side of Eq. (9) (in the following *lhs*) depends only on the geometric co-ordinates of the minima and on the Strouhal-number Sr. A plot of the left hand side versus $\tilde{x}\,Sr$ gives for any arbitrary value of Sr an asymptotic value for large values of $\tilde{x}$, Fig. 3. This asymptotic value depends only on the relative modulation amplitude. The limit for large $\tilde{x}$ values corresponds to a limit for large $[\tilde{\vartheta} - \tilde{\tau}_{min}]$, see Eq. (5). Applying this condition to Eq. (8) yields

$$\varepsilon = -\sin(Sr\,\tilde{\tau}_{min}). \tag{10}$$

This result is used to simplify Eq. (9):

$$lhs = \frac{\tilde{r}(\tilde{\vartheta}, \tilde{\tau}_{min})_{min}^{-2} - 1}{\tilde{x}(\tilde{\vartheta}, \tilde{\tau}_{min})_{min}\, Sr} = \frac{\varepsilon}{(1 - \varepsilon^2)^{3/2}}, \tag{11}$$

which can be solved to yield the modulation amplitude as a function of measurable variables, i. e. of the position of the minima and the frequency (Sr):

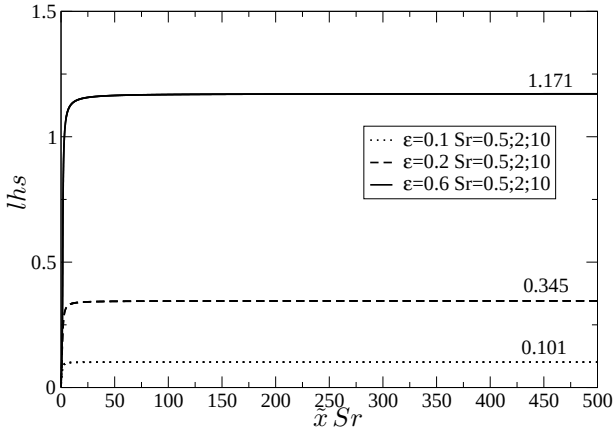

Figure 3: *Asymptotic values of left hand side versus* $\tilde{x}\,Sr$

$$\varepsilon = \left\{ \frac{\sqrt[3]{-108\,lhs + 12\sqrt{3}\sqrt{4 + 27\,lhs^2}}}{6\,lhs} - \frac{2}{lhs\sqrt[3]{-108\,lhs + 12\sqrt{3}\sqrt{4 + 27\,lhs^2}}} + 1 \right\}^{1/2} . \quad (12)$$

Since Eq. (12) is valid only asymptotically, the jet minima should be at a distance from the nozzle of at least $x/r_0 = 4$. Furthermore, the distance should be not much more than $x/r_0 = 15$ because the influence of the surface tension, which has been neglected in the theory, increases with distance. The maximal error of ε obtained from Eq. (12) is 5.8%. With the knowledge of the value of ε and the associated actuator voltage U_a one obtains a gauge function $\varepsilon = f(U_a)$ for discrete frequencies.

RESULTS

Initially a large number of measurements were performed to find all possible different jet structures. They can be classified into at least nine categories which are shown in Chaves et al. [2]. In previous investigations the quantitative knowledge of the modulation amplitude was uncertain. With its here introduced quantitative description a more detailed analysis in the non-dimensional space became possible.

Although all these phenomena differ from each other, continuous transitions are observed, [3]. It is evident that one of the basic parameters is the modulation amplitude. If the amplitude is too small no structures can be generated. Rayleigh´s theory [4] predicts that in the range $Sr > 1$, where the wave length is shorter than the circumference of the jet, perturbations are damped. Consequently, Sr seems to be the next important parameter. In Fig. 4 the occurrence of the main structures are shown in an ε-Sr plane. For better understanding, additional lines are sketched. To guarantee a continuous outflow of the liquid a theoretical upper limit of $\varepsilon = 1$ is conceivable. The gap at the upper left corner of Fig. 4 is caused by the limitations of the experimental set-up to obtain large velocity fluctuation u' at low frequencies. The analysis of experiments with $Sr < 1$ is hardly possible because the optical access of the present set-up is restricted to an area near the nozzle exit. The lower

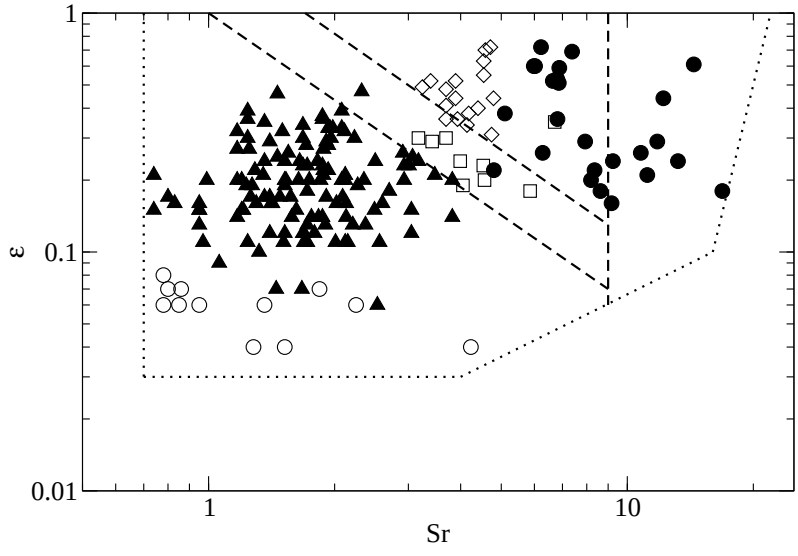

Figure 4: *Observed structures in* ε*-Sr plane:* ○ *waves,* ▲ *upstream directed bells,* □ *discs,* ◊ *downstream directed bells and* • *droplet chains*

horizontal line and its continuation represent the minimal modulation needed to overcome surface forces at the nozzle exit, i. e. for structures to appear. However, also structures generated by a modulation amplitude slightly above the lower horizontal line are damped further downstream. Below this limit the disturbances are damped according to linear theory if $Sr > 1$. The limit, above which wave amplification can be observed for $Sr > 1$, is around $\varepsilon = 0.07$. Although this result has been obtained for laminar jets it implies that turbulent velocity fluctuations are sufficient to initiate the atomization of a jet. The vertical dashed line of Fig. 4 denotes a limit of $Sr = 9$ above which only droplet chains are observed. The oblique dashed lines on Fig. 4 delimit the area where discs occur. Discs can be seen as transition structure between upstream and downstream directed bells.

Since this area is located obliquely in the ε-Sr plane the mentioned transition can obtained by variation of Sr and/or of ε.

In Fig. 5 series of pictures are shown exemplarily. The first row are measurements chosen to have nearly the same modulation amplitude of about $\varepsilon = 0.29$ and Sr is varied. Exactly the same values are not always possible because the dimensionless numbers depend simultaneously on several experimental values. The next row displays structures for approximately constant $Sr \approx 3.5$. Qualitatively, the transition between the structures can be seen.

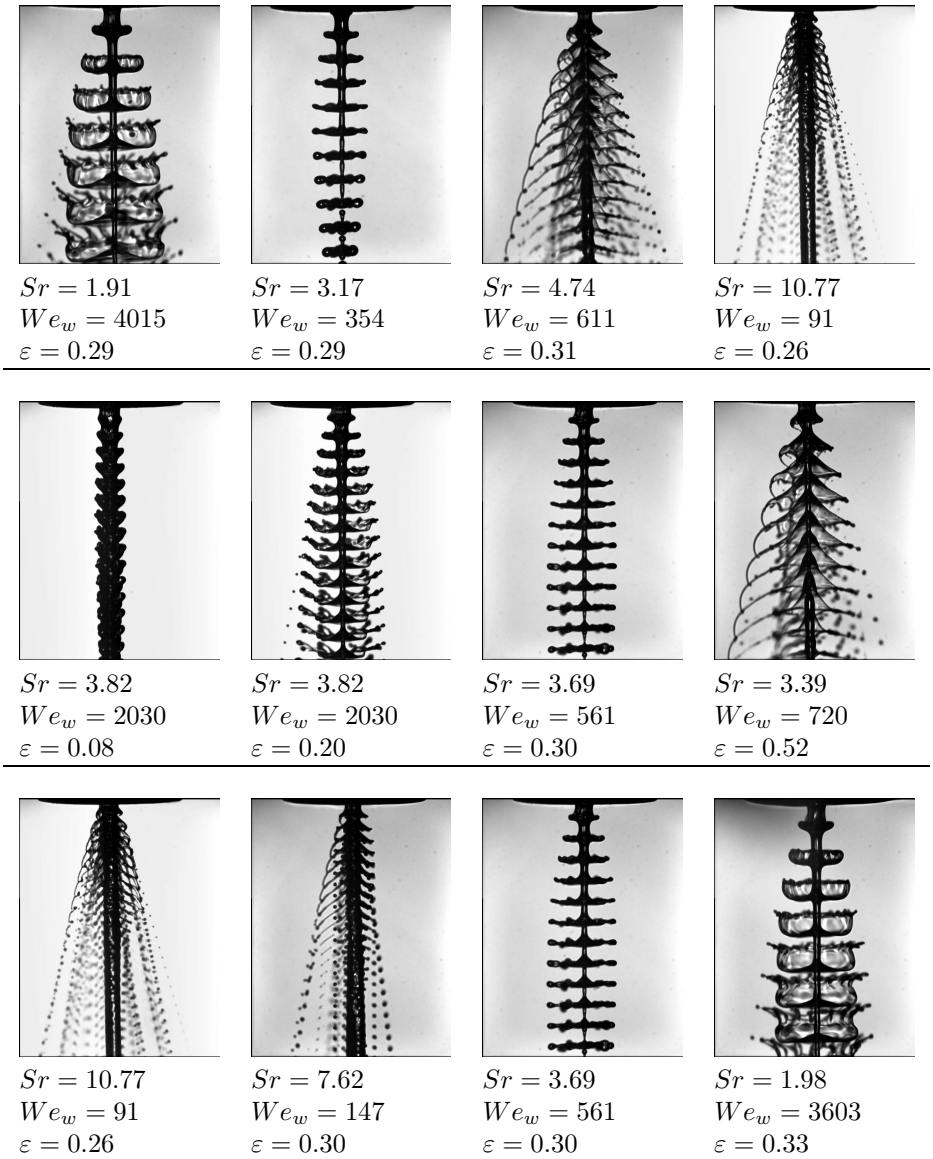

Figure 5: *Transition between different phenomena; test liquid ethanol; Top row: ε is nearly constant, Sr has been varied. Second row: Sr has been held constant, ε has been varied. Bottom row shows the transition at different We_w-numbers and nearly constant ε.*

Next the effect of surface tension on the stability of the jets is observed by varying the Weber-number We_w. The results displayed in Fig. 6 are very useful in delimiting the structures from each other. For values of We_w lower than 200 there are only droplet chains. A significant development of large structures is suppressed and droplet chains are generated directly. The droplet chains seems to be the only phenomenon which doesn't changes into another one for decreasing We_w and ε. The corresponding minimal modulation amplitude is about $\varepsilon = 0.15$. In the adjacent range for $200 < We_w < 1000$ the structures change to discs and downstream directed bells. However, there is a sharp limit between them around $\varepsilon = 0.3$. While above $\varepsilon = 0.3$ downstream directed bells are observed there are only discs for $0.15 < \varepsilon < 0.3$. The range $We_w > 1000$ contains upstream directed bells and waves. Since waves are structures of low modulation amplitude they are damped below a critical value of $\varepsilon \approx 0.07$.

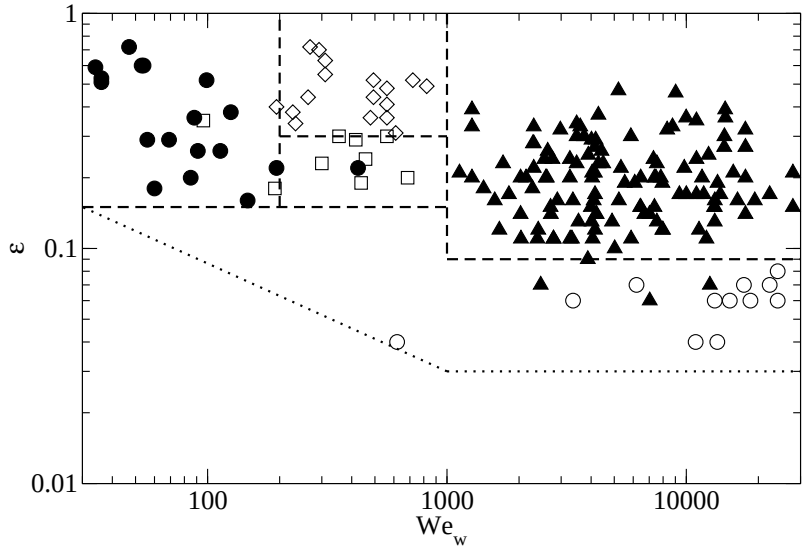

Figure 6: *Observed structures in ε-We_w plane: ○ waves, ▲ upstream directed bells, □ discs, ◊ downstream directed bells and • droplet chains*

CONCLUSIONS

Atomization is influenced by several physical parameters. The number of these parameters has been reduced by using dimensional analysis to five dimensionless parameters. It is assumed that the behaviour of a modulated jet can be described by these parameters. A very important step concerning the quantitative evaluation of the experimental results was the derivation of the dependency between the actuator voltage and the resulting relative modulation amplitude which is an essential parameter. With the help of the set of dimensionless parameters all observed phenomena could be classified and delimited from each other. For a sufficiently high modulation amplitude ($\varepsilon > 0.07$) waves with short wave length ($Sr > 1$) are amplified and lead to atomization in a deterministic manner.

NOMENCLATURE

A_{nozzle}	[m^2]	cross section of the nozzle
D	[m]	diameter of the nozzle
f	[s^{-1}]	modulation frequency
Δp	[Pa]	pressure difference
r	[m]	jet radius
t	[s]	time
u	[m/s]	velocity in jet direction
u'	[m/s]	velocity fluctuation
$\bar{u}$	[m/s]	mean jet velocity
U_a	[V]	actuator voltage
$\dot{V}$	[m^3/s]	flow rate
x	[m]	jet co-ordinate
ζ	[-]	pressure loss factor
ϑ	[-]	non-dimensional time
λ	[m]	wave length of modulation
ν	[m^2/s]	kinematic viscosity
ϱ_{gas}	[kg/m^3]	gas density
ϱ_{liquid}	[kg/m^3]	liquid density
σ	[N/m]	surface tension
τ	[-]	non-dimensional time

Subscripts

0	origin of the jet
min	minima of jet radius
w	wavelength of modulation

REFERENCES

[1] G. Grabitz, Berechnung pulsierender Flüssigkeitsfreistrahlen, Report 15/1990, Max–Planck–Institut für Strömungsforschung, Göttingen, 1990

[2] H. Chaves and F. Obermeier and T. Seidel and V. Weise, Fundamental investigation of the disintegration of a sinusoidally forced liquid jet, *Proc. 8th ICLASS*, Pasadena, pp. 1018–1024, 2000

[3] F. Geschner and F. Obermeier and H. Chaves, Investigation of different phenomena of the disintegration of a sinusoidally forced liquid jet, *Proc. 17th ILASS*, Zurich, pp. 310–314, 2001

[4] L. Rayleigh, On the instability of jets, *Math. Soc. Proc. London*, vol. 10, pp. 4–13, 1878